Ultimately Simple One-pot Single-step Synthesis of Rare Earth Doped Spherical Mesoporous Metal Oxide Nanospheres with Upconversion Emission Ability in Supercritical Methanol

Pengyu Wang[a,*], Kazuya Yokoyama[a], Tomoya Konishi[b], Nagatoshi Nishiwaki[a], Kazuya Kobiro[a,*]

[a] *School of Environmental Science and Engineering, Kochi University of Technology, 185 Miyanokuchi, Tosayamada, Kochi 782-8502, Japan*

[b] *Center for Collaborative Research, Anan National College of Technology, 265 Aoki Minobayashi, Anan, Tokushima 774-0017, Japan*

Graphical abstract

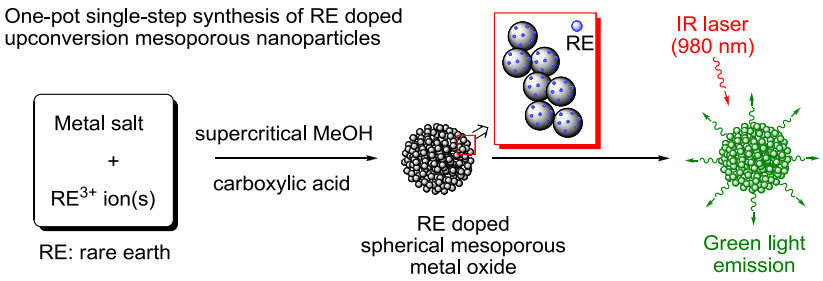

*Corresponding author. Tel.: +81 887 57 2503; fax: +81 887 57 2520.

E-mail address: wang.pengyu@kochi-tech.ac.jp (P. Wang);

kobiro.kazuya@kochi-tech.ac.jp (K. Kobiro)

ABSTRACT

Rare earth doped spherical mesoporous metal oxide nanospheres with upconversion emission ability and large surface area were successfully synthesized by a rapid one-pot single-step method. The reaction medium comprised supercritical methanol with carboxylic acid as an organic additive. Mesoporous Er doped CeO_2 and Er and Yb co-doped CeO_2 nanospheres emit green light under even low-power IR laser irradiation (980 nm, 10 mW) without calcination. Stronger intensity was achieved by high-temperature calcination. Spherical mesoporous nanoparticles were successfully doped with other metals and nitrogen to form TiO_2:Eu, TiO_2:Ce, TiO_2:Yb, TiO_2:Fe, and TiO_2:N according to the similar procedure combining supercritical methanol.

Keywords: One-pot single-step synthesis, Rare earth doping, Spherical mesoporous metal oxide, Upconversion emission, Supercritical methanol

1. Introduction

Rare earth (RE) doped upconversion (UC) fluorescent ceramic nanoparticles (NPs) form a novel class of nonlinear optical materials that absorb photons from long-wavelength light to emit short-wavelength visible light. The properties of RE doped UCNPs include high chemical stability, low toxicity, and higher signal-to-noise ratio than quantum dots and organic dye markers, especially *in vivo* [1,2]. Consequently, these NPs have attracted much attention for their potential applications in optical communications, optoelectronic devices, flat panel displays, photodynamic therapy, and biosensors [3-10]. Several RE dopants, such as Er^{3+} [11-16], Eu^{3+} [17-19], Sm^{3+} [20,21], Tm^{3+} [22], and Ho^{3+} [23], have been utilized as luminescent centers. To reduce multiphonon relaxation and concentration quenching, the host materials of the UCNPs fixing the dopant in the appropriate position should be carefully selected. Metal oxides are one of the best host materials for RE ions because many of them, such as CeO_2, ZrO_2, TiO_2, etc. are highly transparent to visible light and possess strong mechanical, optical, and thermal stabilities and properties [11-22]. Dimension-controlled spherical mesoporous RE doped UCNPs are especially preferred for applications *in vivo*. Their spherical porous structure, ease of manipulation, mono-dispersive nature, and enhanced

light-harvesting capacity renders them ideally suited for drug delivery, cell markers, and photodynamic therapy [3-10,24,25]. Several methods have been reported for the synthesis of spherical mesoporous RE doped UCNPs. However, almost all of these methods involve multi-step reactions.

We have designed and synthesized a new category of spherical mesoporous (metal) oxide NPs termed **m**esoporously **a**rchitected, **r**oundly **i**ntegrated **m**etal **o**xides (MARIMO) NPs because their shapes resemble those of *MARIMO* (*Cladophora aegagropila*) moss balls [26,27]. We have reported an ultimately simple synthetic method for producing spherical mesoporous (metal) oxide NPs, such as SiO_2, TiO_2, ZrO_2, and CeO_2 [26,27]. The method is based on "one-pot single-step reaction" of a mixture containing metal salt and carboxylic acid as a precursor and an organic additive, respectively, in supercritical alcohol. The reaction time is very short (<10 min) [26,27]. Mesoporous spherical NPs have been successfully adopted in biolistic bombardment (gene-delivery) of DNA [27]. By appropriately designing the reaction conditions, we can introduce additional materials such as Er^{3+}, Eu^{3+}, Yb^{3+}, and Ce^{3+} as dopants into the reaction mixture. This process yields RE doped MARIMO NPs and some of them should emit visible light under IR laser excitation. In this paper, we present a novel

approach for obtaining mesoporous spherical RE doped NPs with UC fluorescence ability, by one-pot single-step reaction in supercritical methanol (scMeOH).

2. Materials and methods

2.1 General information

Cerium(III) nitrate hexahydrate, zirconium(IV) oxynitrate dehydrate, titanium tetraisopropoxide, erbium(III) acetate tetrahydrate, ytterbium(III) acetate hydrate, europium acetate hydrate, cerium(III) acetate monohydrate, iron(III) nitrate nonahydrate, methanol, formic acid, acetic acid, phthalic acid, benzoic acid, and benzamide were purchased from Wako Pure Chemical Industries Co. Ltd. They were used as received without further purification.

2.2 Characterization

XRD patterns were obtained using Rigaku SmartLab with graphite-monochromatized Cu $K\alpha$ radiation. Transmission electron microscopy (TEM) and high-resolution transmission electron microscopy images were taken using JEOL JEM-2100F. EDX mapping and spectra were obtained from Oxford Inca Energy TEM 250. Field emission scanning electron microscope images were taken on Hitachi S-5500.

Photoluminescence spectra were obtained on Hitachi High-technologies F-7000. FTIR spectra were taken on JASCO FT/IR-4200. DLS analyses were performed on Photal FPAR-1000. Nitrogen adsorption–desorption isotherm spectra were obtained using BEL Japan INC Belsorp II, and BET specific surface areas were obtained using BET Shimadzu FlowSorb II 2300. Ultraviolet visible absorption spectroscopy (UV-vis) spectra of the nanoparticles were obtained on JASCO V-670 and UV-vis spectra of the solvent were obtained on JASCO V-560.

2.3 Syntheses

Metal salt (2 mmol) and an appropriate amount of a dopant precursor were added to a solution of carboxylic acid (HCOOH, CH_3COOH, phthalic acid, or benzoic acid) in 20 mL of methanol (MeOH) (0.5 or 1.0 mol L^{-1}) with vigorous stirring. The MeOH solution of the precursor dopant, carboxylic acid, and metal salt (3.5 mL) was transferred into an SUS 316 batch-type reactor (10 mL volume). The reactor was sealed with a screw cap, which was equipped with a thermocouple for measuring the inner reactor temperature. The reactor was then placed in a molten salt bath maintained at an appropriate temperature, and heated for an appropriate time. The reaction was quenched by placing the reactor into an ice-water bath. The screw cap was opened once the

reactor had cooled completely. The crude product was sonicated in MeOH (30 min) and centrifuged (6600 rpm, 10 °C, and 30 min). The upper layer was decanted. This procedure was performed three times. The obtained powdery product was then vacuum-dried at 30 °C for 24 h. The prepared powdery product was calcinated in an electronic oven at 500 or 800 °C for 60 min in air if required.

3. Results and discussion

It is well known that smaller phonon energy causes smaller multiphonon relaxation rates which improve the fluorescence intensity in UP materials [28]. To accomplish low phonon energy and higher emission intensity, a host material with a high atomic weight is used. CeO_2, a high atomic weight compound, is a favored host material. On the other hand, Er^{3+} is typically used as a dopant for UCNPs because it emits green light under IR laser irradiation. Therefore, we first synthesize mesoporous spherical Er^{3+} doped CeO_2 (CeO_2:Er) by treating a homogeneous solution of $Ce(NO_3)_3{\cdot}6H_2O$, $Er(OCOCH_3)_3{\cdot}4H_2O$, and HCOOH (molar ratio 10:1:50) in MeOH under supercritical conditions (300 °C, 10 min, and 0.28 g mL^{-1} MeOH) [29]. From EDX mapping of the obtained Er^{3+} doped CeO_2, CeO_2:Er (10:1) [30] MARIMO NPs, the Er atom is found to be dispersed homogeneously throughout the CeO_2 NPs. The Er content in the NPs was determined as 3.2 mol% by elemental analysis on EDX (Fig. 1a, 2c, S1, and S2) [31]. In addition, the XRD pattern of CeO_2:Er (10:1) was identical to that of the prototype CeO_2 NPs. Given these data, we expect that Er atoms are embedded in the crystal lattice. However, the NPs never fluoresced under excitation by a low-intensity IR laser (980 nm, 10 mW) even after calcination. The likely cause of this phenomenon is concentration quenching. Therefore, we reduced the content of Er in the CeO_2:Er MARIMO NPs and performed a

similar treatment of a homogeneous solution of $Ce(NO_3)_3 \cdot 6H_2O$, $Er(OCOCH_3)_3 \cdot 4H_2O$, and HCOOH (100:1:500) in MeOH under the supercritical conditions. This process yielded particles of CeO_2:Er (100:1), which appear to be MARIMO particles (Fig. 1b and S3). The morphology of the secondary MARIMO was unaltered by calcination (TEM; Fig. 1b, c, and S3). The cubic crystal structures of the particles were also preserved after calcination (XRD; Fig. 2b and c). However, calcination reduced the diameter of the secondary MARIMO NPs by 20% (Fig. S4). The lattice constants decreased with the calcination temperature, whereas the primary single crystal size was enlarged after calcination (Fig. S5). These phenomena can be explained by sintering [32], whereby small primary single crystals can diffuse across the boundaries and fuse together to form larger one. The total MARIMO NPs' volume decreased because MARIMO NPs can be densely packed with the elimination of pores. On the other hand, the lattice constant decreased can be due to the evacuation of interstitial protons by heating. As shown in Fig. 5, the absorption band by O-H stretching vibration decreased after calcination process in the FTIR spectra, which indicate that the dehydration of particles would occur by calcination. Therefore, the proton evacuation may take place in the process of ion diffusion of sintering. Brunauer-Emmett-Teller (BET) specific surface

area of the calcinated NPs (800 °C) is 15.3 m^2 g^{-1} and their pores are 2-15 nm mesopores (Fig. 3a and b).

Fig. 1

Fig. 2

Fig. 3

Importantly, the obtained particles emitted green light under low-intensity IR laser irradiation (980 nm, 10 mW) even without calcination. Photoluminescence spectra of the irradiated NPs reveal two emission bands at around 550 nm (green) and 680 nm (red) attributable to $^2H_{11/2}$,$^4S_{3/2}\rightarrow{}^4I_{15/2}$ and $^4F_{9/2}\rightarrow{}^4I_{15/2}$ emissions of Er^{3+}, respectively (Fig. 4a). As expected, both intensities improved following calcination at 500 °C for 60 min and further improved at 800 °C for 60 min (Fig. 4b and c, respectively). In addition, the Fourier transform IR (FTIR) spectra were obtained to know the organic residue in the MARIMO NPs. The broad absorptions appeared at 3700-3000 cm^{-1} consistent with hydrogen-bonded O-H stretching on the surface of primary NPs in the CeO_2:Er (100:1) MARIMO NPs [33,34]. The absorptions at 1650–1550 and 1410 cm^{-1} correspond to absorptions of the carboxylate (COO^-) group [33,34], indicating that carboxylic acid is attached to the surface of the primary NPs in CeO_2:Er (100:1) MARIMO NPs (Fig. 5a). The absorption losses were observed in the FTIR spectra after calcination at 500 and

800 ºC (Fig. 5b and c, respectively). In fact, NPs calcinated at 800 ℃ for 60 min lost 5% of their original weight, indicating removal of organic residues and/or water from the surface of the primary NPs in the MARIMO NPs.

Fig. 4

To test the versatility of the one-pot one-step synthetic procedure, a second dopant, Yb, was co-doped with Er [35]. A homogeneous solution of $Ce(NO_3)_3 \cdot 6H_2O$, $Er(OCOCH_3)_3 \cdot 4H_2O$, $Yb(OCOCH_3)_3 \cdot nH_2O$, and HCOOH (100:1:1:500) in MeOH under the supercritical conditions easily yielded Yb co-doped CeO_2:Er MARIMO NPs, CeO_2:Er,Yb (100:1:1) [30] (Fig. 1e, 1f, and S7) [29]. EDX mapping of CeO_2:Er,Yb (10:1:1) [30,31] reveals the homogeneous distribution of 3.0 mol% of Er and 3.1 mol% of Yb throughout the MARIMO NPs (Fig. 1d, S8, and S9). XRD measurements indicate a cubic crystal structure that was preserved after calcination (Fig. 4d, e, and f). The NP pore of the calcinated NPs was classified as mesopores with 2–15 nm diameter, and the BET specific surface area was 16.0 $m^2\ g^{-1}$ (Fig. 3c and d). Calcination removed all organic residues (Fig. 4d and e). Moderately strong green light emission from the prepared NPs was observed by the naked eye under low-intensity IR laser irradiation (980 nm; 10 mW), even in noncalcinated samples (Fig. S10a). Calcination well enhanced the emission intensities, as anticipated (Fig. S10b). Similar to the prototype

CeO_2:Er NPs, two emission bands were observed at around 550 and 680 nm in the photoluminescence spectra of the NPs (Fig. 4d and e). Emission intensity was stronger in the red than in the green region because of efficient energy transfer from the Yb co-dopant to the Er luminescence center [35]. These results show that Yb co-doped CeO_2:Er MARIMO NPs with efficient UC emission ability were successfully prepared by one-pot single-step reaction in scMeOH. To our knowledge, the NPs reported in the previous papers always require calcination processes for emission [11-16]. However, in our case, the calcination process is not necessary for the energy UC emission even under low power IR laser irradiation (980 nm, 10 mW), which could be due to the unique light harvesting property of mesoporous structure of the MARIMO NPs [24,25]. When mesoporous NPs is irradiated by light, the mesopores allow the light to scatter to inside of pore channels and make multiple reflection between the primary particles. As a result, the pores can exhibit light harvest effect which makes the light absorption much efficient as compare to the normal NPs. [24,25]. On the other hand, the mesoporous structure of the MARIMO NPs with energy UC ability can be very suitable for carrying drugs or sensitizers for the drug delivery or photodynamic therapy.

The one-pot single-step simultaneous doping approach is applicable to other metal oxide NPs. We prepared Er^{3+} doped ZrO_2:Er (200:1) and TiO_2:Er (200:1) [31]

MARIMO NPs [30] using a similar method at 400 °C in scMeOH, [29] which have lower atomic weights than Ce (ZrO_2:Er, Fig. 1g-i, 2g-i, and 3e-f; TiO_2:Er, 1j-l, 2j-l, and 3g-h) [29,31]. Although neither ZrO_2:Er (200:1) nor TiO_2:Er (200:1) emitted green light under low-intensity IR laser (980 nm, 10 mW) prior to calcination, the calcinated versions of both NPs emitted green light despite the lighter atoms comprising the host matrixes (Fig. S15 and S19) [36,37].

Using a similar procedure in scMeOH, we synthesized additional MARIMO NPs doped with metals, TiO_2:Eu (10:1), TiO_2:Ce (10:1), TiO_2:Yb (10:1), and TiO_2:Fe (10:1) [29]. The EDX mapping images, XRD patterns, and EDX spectra clearly indicate that anatase MARIMO TiO_2 NPs were homogenously doped with Eu, Ce, Yb, and Fe (Fig. 6). In addition, a mixture of benzamide and benzoic acid in scMeOH yielded nitrogen doped TiO_2 MARIMO NPs [29]. These NPs remained yellow even after calcination at 500 ℃ for 60 min in air (Fig. S25). Their absorption starts in the visible region (480 nm; Fig. 27), suggesting their suitability as a visible light photocatalyst. Indeed, MARIMO TiO_2:N irradiated by 460 nm visible light degraded methylene blue in water with almost no absorption observed within 120 min. The reaction rate constant was k_f = 1×10^{-2} min^{-1}.

Fig. 5

Fig. 6

Considering the formation mechanism, we have proposed a carboxyl-group-assisted process for the formation of MARIMO NPs in the previous papers [26,27]. Here, we propose a similar reaction mechanism for the one-pot single-step synthesis of RE doped spherical mesoporous metal oxide NPs in scMeOH (Scheme 1). When the homogeneous and transparent methanol solution of metal salt, carboxylic acid, and RE salt was treated under scMeOH conditions, esterification of acids with methanol proceeds easily with water formation. The metal oxide was produced by the reaction of metal salt with the water followed by dehydration. On the other hand, the metal element could be substituted by RE element simultaneously to dope the RE element in the metal oxide crystal. Parallel decomposition of the carboxylic acid evolves gaseous products such as CO_2 and hydrocarbons. The resulting RE doped metal oxide aggregates grow and swell to form a mesoporous structure MARIMO NPs.

Scheme 1

4. Conclusions

In summary, RE doped spherical mesoporous metal oxide UC fluorescent NPs, such as CeO_2:Er, CeO_2:Er,Yb, ZrO_2:Er, and TiO_2:Er MARIMO NPs, with large surface areas were successfully synthesized by a rapid, ultimately simple, and facile one-pot single-step method in the presence of carboxylic acid in scMeOH. Our synthetic approach proved to be a highly versatile means of producing mesoporous spherical metal oxide NPs doped with (metallic) elements. Clear green light emission was confirmed even under weak IR laser irradiation (980 nm, 10 mW) without calcination. Adequately strong fluorescence intensity was achieved not merely from calcinated CeO_2:Er NPs but also from CeO_2:Er,Yb MARIMO NPs. The applications of these metal-doped MARIMO NPs to photodynamic therapy and their potential use as biosensors and catalysts will be published elsewhere.

Acknowledgements

The authors are sincerely grateful to Prof. Hiromichi Aono of Ehime University for the BET and nitrogen adsorption–desorption isotherm spectra. The authors thank Dr. Noriko Nitta of Kochi University of Technology for her fruitful discussions. The authors also thank Mr. Tetsuo Nagayama and Mr. Masato Sato of social cooperation division of Kochi University of Technology for their support.

References

[1] Z. Xu, P. Ma, C. Li, Z. Hou, X. Zhai, S. Huang, J. Lin, Monodisperse core–shell structured up-conversion $Yb(OH)CO_3@YbPO_4:Er^{3+}$ hollow spheres as drug carriers, Biomaterials 32 (2011) 4161–4173;

[2] C. Li, J. Lin, Rare earth fluoride nano-/microcrystals: synthesis, surface modification and application, J. Materials Chemistry 20 (2010) 6831–6847.

[3] N.M. Idris, M.K. Gnanasammandhan, J. Zhang, P.C Ho, R. Mahendran, Y. Zhang, In vivo photodynamic therapy using upconversion nanoparticles as remote-controlled nanotransducers, Nature Medicine 18 (2012) 1580–1585.

[4] M.E. Lim, Y.-L. Lee, Y. Zhang, J.J.H. Chu, Photodynamic inactivation of viruses using upconversion nanoparticles, Biomaterials 33 (2012) 1912–1920.

[5] M. Haase, H. Schäfer, Upconverting nanoparticles, Angewandte Chemie International Edition 50 (2011) 5808–5829.

[6] J.-C.G. Bünzli, Lanthanide luminescence for biomedical analyses and imaging, Chemical Reviews 110 (2010) 2729–2755.

[7] S.V. Eliseeva, J.-C.G. Bünzli, Lanthanide luminescence for functional materials and bio-sciences, Chemical Society Reviews 39 (2010) 189–227.

[8] F. Wang, X. Liu, Recent advances in the chemistry of lanthanide-doped upconversion nanocrystals, Chemical Society Reviews 38 (2009) 976–989.

[9] T. Konishi, M. Shimizu, Y. Kameyama, K. Soga, Fabrication of upconversion emissive LaOCl phosphors doped with rare-earth ions for bioimaging probes, Journal of Materials Science: Materials in Electronics, 18 (2007) S183–S186.

[10] F. Auzel, Upconversion and anti-stokes processes with f and d ions in solids, Chemical Reviews 104 (2004) 139–173.

[11] P. Zhao, Y. Zhu, X. Yang, K. Fan, J. Shen, C. Li, Facile synthesis of upconversion luminescent mesoporous Y_2O_3:Er microspheres and metal enhancement using gold nanoparticles, RSC Advances 2 (2012) 10592–10597.

[12] W. Luo, C. Fu, R. Li, Y. Liu, H. Zhu, X. Chen, Er^{3+}-doped anatase TiO_2 nanocrystals: crystal-field levels, excited-state dynamics, upconversion, and defect luminescence, Small 7 (2011) 3046–3056.

[13] X. Chen, W. Luo, Optical spectroscopy of rare earth ion-doped TiO_2 nanophosphors, J. Nanoscience Nanotechnology 10 (2010) 1482–1494.

[14] S. Jeon, P.V. Braun, Hydrothermal Synthesis of Er-doped luminescent TiO_2 nanoparticles, Chemistry of Materials 15 (2003) 1256–1263.

[15] A. Patra, C.S. Friend, R. Kapoor, P.N. Prasad, Fluorescence upconversion properties of Er^{3+}-doped TiO_2 and $BaTiO_3$ nanocrystallites, Chemistry of Materials 15 (2003) 3650–3655.

[16] A. Patra, C.S. Friend, R. Kapoor, P.N. Prasad, Upconversion in Er^{3+}:ZrO_2 nanocrystals, J. Physical Chemistry B 106 (2002) 1909–1912.

[17] J. Yin, L. Xiang, X. Zhao, Monodisperse spherical mesoporous Eu-doped TiO_2 phosphor particles and the luminescence properties, Applied Physics Letters 90 (2007) 113112.

[18] B. Julián, R. Corberán, E. Cordoncillo, P. Escribano, B. Viana, C. Sanchez, One-pot synthesis and optical properties of Eu^{3+}-doped nanocrystalline TiO_2 and ZrO_2, Nanotechnology 16 (2005) 2707–2713.

[19] A. Conde-Gallardo, M. García-Rocha, I. Hernández-Calderón, R. Palomino-Merino, Photoluminescence properties of the Eu^{3+} activator ion in the TiO_2 host matrix, Applied Physics Letters 78 (2001) 3436–3438.

[20] M. Ishii, B. Towlson, N. Poolton, S. Harako, X. Zhao, S. Komuro, B. Hamilton, Effects of oxidization and deoxidization on charge-propagation dynamics in rare-earth-doped titanium dioxide with room-temperature luminescence, J. Applied Physics 111 (2012) 053514.

[21] L. Li, C.-K. Tsung, Z. Yang, G.D. Stucky, L. Sun, J. Wang, C. Yan, Rare-earth-doped nanocrystalline titania microspheres emitting luminescence via energy transfer, Advanced Materials 20 (2008) 903–908.

[22] A. Patra, P. Ghosh, P.S. Chowdhury, M.A.R.C. Alencar, W. Lozano B., N. Rakov, G.S. Maciel, Red to blue tunable upconversion in Tm^{3+}-doped ZrO_2 nanocrystals, J. Physical Chemistry B 109 (2005) 10142–10146.

[23] Q. Zhan, J. Qian, H. Liang, G. Somesfalean, D. Wang, S. He, Z. Zhang, S. Andersson-Engels, Using 915 nm laser excited Tm^{3+}/Er^{3+}/Ho^{3+}-doped $NaYbF_4$ upconversion nanoparticles for in *vitro* and deeper in *vivo* bioimaging without overheating irradiation, ACS Nano 5 (2011) 3744–3757.

[24] J.H. Pan, Z. Cai, Y. Yu, X.S. Zhao, Controllable synthesis of mesoporous F–TiO_2 spheres for effective photocatalysis, J. Materials Chemistry 21 (2011) 11430–11438.

[25] J.H. Pan, X. Zhang, A.J. Du, D.D. Sun, J.O. Leckie, Self-etching reconstruction of hierarchically mesoporous F-TiO_2 hollow microspherical photocatalyst for concurrent membrane water purifications, J. American Chemical Society 130 (2008) 11256–11257.

[26] P. Wang, K. Kobiro, Ultimately simple one-pot synthesis of spherical mesoporous TiO_2 nanoparticles in supercritical methanol, Chemistry Letters 41 (2012) 264–266.

[27] P. Wang, K. Ueno, H. Takigawa, K. Kobiro, J. Supercritical Fluids in press.

[28] K. Soga, W. Wang, R.E. Riman, J.B. Brown, K.R. Mikeska, Luminescent properties of nanostructured Dy^{3+}- and Tm^{3+}-doped lanthanum chloride prepared by reactive atmosphere processing of sol-gel derived lanthanum hydroxide, J. Applied Physics 93 (2003) 2946–2951.

[29] Details are shown in Electronic Supplementary Data.

[30] Mole ratio of host metal oxide to dopant in the reaction mixture.

[31] We prepared two types of RE doped MARIMO NPs, since reciprocal high and low concentrations of RE on MARIMO metal oxide NPs are necessary for EDX mapping and photoluminescence, respectively.

[32] R. M. German, Sintering Theory and Practice, John Wiley & Sons, Inc. 1996.

[33] M. Taguchi, S. Takami, T. Adschiri, T. Nakane, K. Sato, T. Naka, Supercritical hydrothermal synthesis of hydrophilic polymer-modified water-dispersible CeO_2 nanoparticles, CrystEngComm 13 (2011) 2841-2848.

[34] Z. Zhang, X. Zhong, S. Liu, D. Li, M. Han, Aminolysis route to monodisperse titania nanorods with tunable aspect ratio, Angewandte Chemie International Edition 44 (2005) 3466-3470.

[35] J. Silver, M.I. Martinez-Rubio, T.G. Ireland, G.R. Fern, R. Withnall, The effect of particle morphology and crystallite size on the upconversion luminescence properties of erbium and ytterbium co-doped yttrium oxide phosphors, J. Physical Chemistry B 105 (2001) 948.

[36] Z. Yang, K. Zhu, Z. Song, D. Zhou, Z. Yin, J. Qiu, Preparation and upconversion emission properties of TiO_2 :Yb, Er inverse opals, Solid State Communications 151 (2011) 364–367.

[37] N.V. Gaponenko, D.M. Unuchak, A.V. Mudryi, G.K. Malyarevich, O.B. Gusev, M.V. Stepikhova, A.P. Stupak, S.M. Kleshcheva, M.I. Samoilovich, M.Yu. Tsvetkov, Modification of erbium photoluminescence excitation spectra for the emission wavelength 1.54 μm in mesoscopic structures, J. Luminescence 121 (2006) 217–221.